Starburst in the Intragroup Medium of Stephan's Quintet[1]

Cong Xu

Infrared Processing and Analysis Center, Jet Propulsion Laboratory, Caltech 100-22, Pasadena, CA 91125

Richard Tuffs

Max-Planck-Institut für Kernphysik, Postfach 103980, D69117 Heidelberg, Germany

Received July 24, 1998; accepted August 25, 1998

[1]Based on observations made with ISO, an ESA project with instruments funded by ESA Member States and with the participation of ISAS and NASA.

ABSTRACT

Based on new ISO mid-infrared observations and ground based H_α and near-infrared observations, we report the detection of a bright starburst in the intragroup medium (IGM) of the famous compact group of galaxies Stephan's Quintet (Source A in Fig.1). We demonstrate that this starburst is caused by a collision between a high velocity (δV$\sim$ 1000 km/sec) intruder galaxy (NGC7318b) and the IGM of the group. While this is the only starburst known today that is induced by a galaxy/cold-intergalactic-medium collision, it provides new constraints to the theory for interaction-induced starbursts, and may hint at a new mechanism for the star formation excess seen in more distant clusters.

Subject headings: galaxies: interactions – galaxies: intergalactic medium – galaxies: ISM – galaxies: starburst – galaxies: active – infrared: galaxies – stars: formation

1. Introduction

Starbursts (Rieke et al. 1980; Gehrz et al 1983) are "cosmic fireworks" where hundreds of thousands of massive stars that are up to a million times brighter than the Sun are born and die in a short time scale of a few 10^7 years (compared to the age of most galaxies of $\sim 10^{10}$ years). Despite the wide interest, many basic questions about starbursts remain unanswered. First of all, how are they triggered? Theoretically the only well established triggering mechanism for starbursts involves low velocity encounters/mergers between galaxies (Larson & Tinsley 1978; Joseph et al. 1984; Lonsdale et al. 1984; Noguchi & Ishibashi 1986; Mihos & Hernquist 1996). In this letter, we shall show that a bright starburst in the intragroup medium (IGM) of the famous compact group of galaxies Stephan's Quintet is triggered by a new mechanism, namely a collision between a high velocity (δV$\sim$ 1000 km/sec) intruder galaxy (NGC7318b) and the IGM of the group.

Stephan's Quintet (hereafter SQ), discovered 120 years ago (Stephan 1877), is perhaps the most famous example of the compact galaxy group class that is characterized by aggregates of 4-8 galaxies with implied space densities as high as those in cluster cores (Hickson 1982). SQ has been observed with almost every large telescope and in almost every domain of the electromagnetic spectrum. These data suggest (Moles et al. 1997) that SQ has been visited by at least two "intruders" (NGC7320c and NGC7318b) in the past few 10^8 years. Consequently, its intragroup medium (IGM) is filled with HI gas stripped from its spiral members (Shostak et al. 1984). In an attempt to study the star formation activity and the dust properties of this IGM we made observations at 11.4μm, 15μm (ISOCAM), 60μm and 100μm (ISOPHT) using the Infrared Space Observatory (Kessler et al. 1996). In these observations, an outstanding bright source (Source A in Fig.1) is detected in a region quite far away from centers of member galaxies. In this letter, we publish the ISOCAM 15μm data (the rest of ISO data will be published in subsequent papers) which, together

with data from the following-up gound based H_α and NIR observations, demonstrate conclusively that this bright source is associated with a starburst in the IGM of SQ.

2. Observations

2.1. ISOCAM observations

The ISOCAM observations at $15\mu m$ (Fig.1) were made on 1996 May 23 using the ISOCAM Long-Wavelength-Channel array (32×32 pixels). Raster scans with $PFOV = 6''$, $M = 12$, $\delta M = 48''$ (in-scan) and $N = 20$, $\delta N = 6''$ (cross-scan) were made in the micro-scan mode (CAM01) using filter LW3 ($\lambda_0 = 15\mu m$, $\delta\lambda = 6\mu m$). The 1σ rms noise measured in the inner part ($\sim 5' \times 3'$) of the image is 0.04 mJy/pixel, and is higher near the edges of the image. The absolute calibration is taken from the ISOCAM Observer's Manual (1994), which has an uncertainty of less than 30% (Sauvage, private communication). The angular resolution (FWHM) of the image is $10''$. The basic data reduction was done using the CAM Interactive Analysis (CIA) software[2].

2.2. H_α observations

The H_α observations (Fig.2) were made in August 1997 using the 2.2m telescope of the observatory of Max-Planck-Institut at Calar Alto (Spain). In order to separate the H_α emission associated with the intruder galaxy NGC7318b ($v \simeq 5700$ km/sec) from the H_α emission associated with the rest of the group ($v \simeq 6600$ km/sec), CCD images of the H_α–[NII] emission were obtained using two narrow band filters 667/7 and 674/8, centered at

[2]CIA is a joint development by ESA Astrophysics Division and the ISOCAM Consortium led by the ISOCAM PI, C. Cesarsky, Direction des Sciences de la Matiere, C.E.A., France.

6667Å and 6737Å with FWHM bandwidths of 66Å and 76Å, respectively. The transmission of the 667/7 filter for the H_α line of redshift 0.019 (v = 5700 km/sec) is 0.49, and for the H_α line of redshift 0.022 (6600 km/sec) is 0.04. The transmissions of the 674/8 filter for the same two components of the H_α emission are 0.06 and 0.49, respectively. The 5700 km/sec component of the H_α–[NII] emission is therefore estimated from the image obtained using the 667/7 filter, and the 6600 km/sec component from the 674/8 image. The continuum in both images is subtracted using an R-band CCD image of the same field. To enhance the sensitivity for the diffuse emission, both H_α–[NII] maps (original resolution $\sim 1''$) are smoothed to a round Gaussian beam with FWHM=2″. Note that in some regions the two components have similar morphology. This could be an indication that the emission in those regions is rather associated with another component, namely the one with recession velocity of 6000 km/sec (Moles et al. 1997; Shostack et al. 1984). However this uncertainty does not affect seriously the H_α fluxes (which are sums of the 5700 km/sec and the 6600km/sec components) reported in Table 1, because while the 6000km/sec component might have been counted twice, its flux would have been underestimated by about a factor of two in both the 667/7 map and the 674/8 map, given that the transmissions of the two filters for the 6000 km/sec component are only about half of the transmissions for the 5700 km/sec and the 6600 km/sec component, respectively.

2.3. Near Infrared K'-band observation

A near infrared K'-band ($\lambda_0 = 2.1\mu m$) image of the central part of Stephan's Quintet were obtained using the 3.5m telescope of the observatory of Max-Planck-Institut at Calar Alto (Spain), mounted with the 256×256 pixels (pixel size =0.″81) MAGIC camera. The observations were made in March 1997. The weather conditions were photometric and stellar photometry consistent to $\sim$ 2% throughout the night. The seeing was about 1″. The

image covers about $4' \times 4'$ sky (Fig.2). In the central $3' \times 3'$ field, the 1σ rms noise is 20.4 mag/arcsec^2. Because of the mosaic, the noise is higher near the edges.

3. Results

3.1. A starburst (Source A) far away from galaxy centers

Figure 1 presents the central $\sim 4' \times 4'$ region of the $15\mu m$ ISOCAM image of Stephan's Quintet (false color). As shown by Sauvage et al. (1996), the $15\mu m$ emission is a good, nearly extinction free star formation rate indicator. Located slightly upper-right from the map center, Source A lies about $1'$ ($\sim$ 25 kpc at D = 80 Mpc where H_0=75) north of NGC7318b and about $1'$ west of NGC7319. It covers a region of $\sim 30''$ and its peak surface brightness in the $15\mu m$ map is second only to that of the Sy2 nucleus of NGC7319. At 80Mpc the $15\mu m$ flux density of Source A corresponds to a luminosity (νL_ν) $L_{15\mu} = 4.8\ 10^8 L_\odot$, about 30 times higher than the $L_{15\mu}$ ($1.7\ 10^7 L_\odot$) of the foreground Sd galaxy NGC7320 (assumed to be at 10Mpc; Table 1).

In an early photographic observation including both the H_α emission and the underlying continuum emission, Arp (1973) identified several HII regions in the region of Source A. H_α emission was also detected in the Source A region in a recent published H_α image centered on the Sy2 galaxy NGC7319 (Moles et al. 1997) though Source A falls on the edge of that image and therefore is not fully covered. A grid photometry map for SQ by Schombert et al. (1990) reveals a concentration of very blue data points (B−V= 0.3–0.5) in this region. The H_α knots and blue color provide strong support for an interpretation that the MIR emission is due to dust heated by massive young stars.

In order to firmly establish the starburst nature of Source A, we carried out new H_α and K′ ($2.1\mu m$) imaging observations using an optical CCD and a near-infrared detector

array, respectively (Section 2.2 and 2.3). With two narrow band filters (667/7 and 674/8), the 5700 km/sec component and the 6600 km/sec component of the H_α emission, the former being associated with the current intruder galaxy NGC7318b and the latter with the rest of the group (Table 1), are separated. In Fig.2 the contours of the two H_α components are overlaid on the K′ image. Indeed strong H_α emission from both components is detected in the Source A region, and the position of the H_α peak (associated with the 6600km/sec component) coincides well with that of the $15\mu m$ emission peak. The H_α equivalent line width, EW(H_α), of the region is 115±15Å. Such high EW(H_α) is found only in starbursts (Keel et al. 1985).

The star formation rate (SFR) in the Source A region can be estimated from both the $15\mu m$ and the H_α luminosities. A ratio between flux densities of the $15\mu m$ and of the thermal radio at 6cm $f_{15\mu}/f_{th,6cm} = 85$ (mJy/mJy) is assumed, taken from the median value of the star formation regions in M51 (Fig.2b of Sauvage et al. (1996)). Following Kennicutt et al. (1994) and adopting a Salpeter IMF with $m_l = 0.1$ $M_\odot$ and $m_u = 100$ $M_\odot$, we obtain from Source A's $15\mu m$ luminosity (4.8 10^8 $L_\odot$) an SFR of 0.81 $M_\odot/yr$. Assuming the same IMF, the H_α luminosity (2.2 10^7 $L_\odot$) gives an SFR of 0.66 $M_\odot/yr$. The two estimates of the SFR agree with each other within the uncertainties. This also suggests that the extinction of the H_α emission in Source A is low.

For starbursts, according to Bruzual & Charlot (1993), the stellar-mass to NIR luminosity ratio is insensitive to the starburst age, and therefore the NIR luminosity is a good stellar mass indicator. Using the model of Bruzual & Charlot (1993) and assuming that the stellar population in Source A is the product of a starburst of age 10^7 — 10^8 years (the widely accepted age span of starbursts), the stellar mass in Source A can be estimated from its K′ magnitude (Table 1), which is in the range 0.8 — 1.6 10^7 $M_\odot$. Dividing this mass by the star formation rate derived above, one finds that the starburst in Source A is

only $\sim$ 1—2 10^7 years old. Any possible contribution from an underlying older population (e.g. from stripped stars) may only reduce the estimate of this age, because less NIR light would then be due to stars formed in the current burst.

3.2. Triggering mechanism: IGM–intruder collision

How is the starburst in Source A, which is more than 20 kpc away from centers of nearby galaxies, triggered? HI observations of SQ (Shostak et al. 1984) reveal three velocity components associated with the group (not including the foreground galaxy NGC7320): 1) a 6600km/sec component distributed throughout the intragroup space, 2) a 6000km/sec component north of N7318b and 3) a 5700km/sec component located south of N7318b. Moles et al. (1997) suggested that both the two latter components are associated with NGC7318b, the velocity difference between them due to the rotation. Both the 6600 and 6000 km/sec components show local maxima in the region of Source A, both with HI surface density of $\sim$ 3.3 10^{20} atoms/cm^2. The X-ray (Pietsch et al. 1997) and the radio continuum (van der Hulst & Rots 1981) observations show a shock front, generated by the collision between NGC7318b and the IGM, on the eastern side of NGC7318b (also visible on our H_α maps, Fig.2). Noticeably, Source A is located in a region *without* detected X-ray emission. ROSAT maps (Pietsch et al. 1997) show that Source A lies either: 1) in a gap in the shock related X-ray emission (if the detached emission NW of Source A is interpreted as an extension of the shock front) or 2) on the N edge of the shock front.

The HI, X-ray and radio continuum data in the literature and our MIR, H_α and NIR data are all directing to a scenario such as the following: During the intrusion of NGC7318b into SQ, a high speed ($\sim$ 1000 km/sec) collision between the local maxima of the two HI components in Source A region, one (6600 km/sec component) associated with the intragroup gas and the other (6000 km/sec component) with the intruder NGC7318b,

occurred $\sim 10^7$ years ago. This collision is perhaps part of the larger scale collision which has resulted in the shock front seen in the X-ray and radio continuum observations on the eastern side of NGC7318b. The collision triggers an instantaneous starburst, giving rise to the strong MIR and H_α emission (its $L_{15\mu}$ is about twice of that of the starburst in the collision region of the Antennae Galaxies (Vigroux et al. 1996)). The hot gas produced by the collision has already cooled in the region of Source A presumably due in part to the locally higher gas density which results in a higher cooling rate.

Interestingly, Source A sits also in a region where two long and faint optical arms seemingly run across with each other (Arp & Lorre 1976). Both arms are likely being stretched out from NGC7318b, with the NGC7318a (an early type galaxy, Table 1) in the background/foreground of the western arm (Moles et al. 1997). It is tempting to assume that these arms are products of tidal interactions between NGC7318b and the other two galaxies (NGC7318a and NGC7319), and the starburst in Source A is triggered by the interaction of these two arms of NGC7318b. Strong evidence *against* this scenario, and favoring the IGM–intruder collision scenario, is the presence of a strong 6600km/sec component, which is in fact the dominant component with apparent connection with the shock front, in the H_α emission in Source A (Fig.2). If there is no participation of the IGM in the starburst, the 6600 km/sec component is not at all expected. The fact that the H_α emission in the Source A region is dominated by the 6600km/sec component conclusively demonstrate that most of the star formation in Source A region must be happening in the IGM.

In addition, the time scale for the development of tidal tails is more than a few 10^8 years (Barnes & Hernquist 1992; Elmegreen et al. 1993) while the crossing time of NGC7318b is only a few 10^7 years, too short for the tidal effects to act. Indeed it is more likely that the two optical 'arms' are not 'tidal arms' but are, together with Source A, products of some

hydrodynamical processes induced by the high speed collision between the intruder and the rest of the group. The eastern 'arm' is almost certain to be associated with the shock front (Moles et al. 1997) although the mechanism for the western 'arm' is still not very clear.

Once the IGM environment of the starburst in Source A is determined, the next question is: could it be due to star formation in the cooled gas in the aftermath of the high speed collision, similar to that proposed for the star formation in 'cooling flows' (Fabian et al. 1991)? It has been strongly argued, because of the red colors of the 'cooling flow' galaxies, that if star formation does occur in 'cooling flows' it has to be severely deficient in massive stars (Fabian et al. 1991). This is contrary to what we are seeing in Source A where the high EW(H_α) clearly indicates a starburst with a lot of massive stars. Hence the 'star formation in cooling flow' mechanism is irrelevant here. It is more likely that the starburst in Source A is triggered by the gravitational instability casued by some hydrodynamical processes which in turn are induced by the high velocity collision between the IGM and the intruder. This might have some similatities, albeit in a much larger scale, to the triggering mechanism of the so called 'self-propagating' star formation mode (Blaauw 1964) in the Galactic disk, which is associated with the shocks generated by HII regions (Elmegreen & Lada 1977) and by supernova remnants (Herbst & Assousa 1977).

In summary, our conclusion that the starburst in the Source A region is triggered by the high speed ($\sim$ 1000 km/sec) collision between the IGM and the intruder NGC7318b is supported by the following facts:

1. The H_α data show that the star formation in Source A is occurring both in the IGM (the 6600 km/sec component) and in the intruder (the 5700 km/sec component). In particular, the fact that the H_α emission in the Source A region is dominated by the 6600km/sec component conclusively rules out any interpretation involving only processes confined within the intruder NGC7318b.

2. The age of the starburst ($\sim$ 1— 2 10^7 yrs) estimated from the MIR, H_α and NIR data is consistent with the dynamical time scale of the high speed collision ($\sim 10^7$ yrs). The probability that both the burst and the collision are happening simultaneously (within such a short time scale) would be very low if the former is not causally related to the latter.

3. The HI observations of Shostak et al. (1984) show that both the intragroup gas and the gas associated with NGC7318b have local concentrations in the Source A region. These cold gas components are not only the participants of the high speed collision which triggers the starburst, but also the reservoirs of the necessary material for the starburst to proceed.

4. The morphology of the 6600km/sec component of the H_α emission shows a possible connection between Source A and the shock front, indicating that Source A is likely part of a larger scale collision that is still going on between the IGM and the intruder.

5. Although Source A has no detectable X-ray emission, it is surrounded by X-ray emitting hot gas, again indicating a connection between the shock front (with which the X-ray emitting hot gas is associated) and the starburst. The high pressure imposed by the surrounding hot gas may have also helped sustain the starburst by confining the cold gas in that region.

4. Discussion

4.1. Theoretical implication

Theoretical works on interaction-induced starbursts are still in their early stages (Mihos & Hernquist 1996). Most of the studies have concentrated on the effects of the gravitational tidal force, while the effects of the hydrodynamic shocks generated by the

collision of two gas condensations have been left out (Noguchi & Ishibashi 1986; Mihos et al. 1993). The scenario envisionized by Jog & Solomon (1992) for starbursts induced by low velocity ($\sim$ 100—300 km/sec) galaxy-galaxy collisions is difficult to apply to Source A. In that scenario a starburst occurs when the Giant Molecular Clouds (GMC's) preexisting in the two colliding disks are compressed by the hot shocked gas. In the case of Source A, it is not clear whether the IGM contains GMC's (the CO survey of SQ by Yun et al. (1997) unfortunately did not cover the Source A region). Even if there are indeed preexisting GMC's in the Source A region, the colliding velocity is so high ($\sim$ 600—1000 km/sec) and close to the typical escape velocity in galaxies that the shocked gas may be left behind when the colliding parties move away from each other while GMC's are not affected by the collision because of the low filling factor (Jog & Solomon 1992). Clearly more theoretical work, in particular simulations with a full treatment of gas dynamics, is needed to understand what is going on in starbursts such as Source A.

4.2. A new mechanism for Butcher–Oemler effect?

Events like Source A are very rare in the local universe. However in the earlier universe, in particular in young clusters where high velocity encounters involving late type galaxies are frequent and a large part of the intracluster space may be filled by cold stripped gas, collision between gas rich galaxies and the cold intracluster medium (ICM) may be quite common. Whether the starbursts so induced are at least partially responsible for the enhanced star formation in those young, distant clusters (Butcher & Oemler 1984), needs to be further explored (for an alternative mechanism, see Moore et al. 1996).

We are indebted to Jack Sulentic who helped in the acquisition of H_α data. CX acknowledges very stimulating discussions with Jack Sulentic, and constructive comments of George Helou, Nanyao Lu, and Barry Madore. Part of the work is supported by NASA grant for ISO Data Analysis. NED is supported by NASA at IPAC.

REFERENCES

Arp, H. 1973, ApJ, **183**, 411.

Arp, H. & Lorre, J. 1976, ApJ, **210**, 58.

Barnes, J. & Hernquist, L. 1992, *Nature*, **360**, 715.

Blaauw, A. 1964, ARAA, **2**, 213.

Bruzual, G.A. & Charlot, S. 1993, ApJ, **405**, 538.

Butcher, H. & Oemler, A. 1984, ApJ, **285**, 426.

Elmegreen, B.G. & Lada, C.J. 1977, ApJ, **214**, 725.

Elmegreen, B.G., Kaufman, M. & Thomasson, M. 1993, ApJ, **412**, 90.

Fabian, A.C., Nulsen, P.E.J. & Canizares, C.R. 1991, ARAA, **2**, 191.

Gehrz, R.D., Sramek, R.A. & Weedman, D.W. 1983, ApJ, **267**, 551.

Herbst, W. & Assousa, G.E. 1977, ApJ, **217**, 473.

Hickson, P. 1982, ApJ, **255**, 382.

Jog, C.J. & Solomon, P.M. 1992, ApJ, **387**, 152.

Joseph, R.D., Meikle, W.P.S., Robertson, N.A. & Wright, G.S. 1984, MNRAS, **209**, 111.

Keel, W.C., Kennicutt, R.C., Hummel, E., & van der Hulst, J.M. 1985, AJ, **90**, 708.

Kennicutt, R.C., Tamblyn, P. & Congdon, C.E. 1994, ApJ, **435**, 22.

Kessler, M.F., Steinz, J.A., Anderegg, M.E. et al. 1996, A&A, **315**, L27.

Larson, R.B. & Tinsley, B.M. 1978, ApJ, **219**, 46.

Lonsdale, C.J., Persson, S.E. & Matthews, K. 1984, ApJ, **287**, 95.

Mihos, J.C. Bothun, G.D. & Richstone, D.O. 1993, ApJ, **418**, 82.

Mihos, J.C. & Hernquist, L. 1996, ApJ, **464**, 641.

Mirabel, I.F., Dottori, H. & Lutz, D. 1992, A&A, **256**, L19.

Moles, M., Sulentic, J.W. & Márquez, I. 1997, ApJ, **485**, 69.

Moore, B., Katz, N., Lake, G., Dressler, A., & Oemler Jr, A. 1996, *Nature*, **379**, 613.

Noguchi, M. & Ishibashi, S. 1986, MNRAS, **219**, 305.

Pietsch, W., Trincheri, G., Arp, H. & Sulentic, J.W. 1997, A&A, **322**, 89.

Rieke, G.H., Lebofsky, M.J., Thompson, R.I., Low, F.J. & Tokunaga, A.T. 1980 ApJ, **238**, 24.

Sauvage, M., Blommaert, J., Boulanger, F. et al. 1996, A&A, **315**, L89.

Schombert, J.M., Wallin, J.F. & Struck-Marcell, C. 1990, AJ, **99**, 497.

Shostak, G.S., Sullivan III, W.T. & Allen, R.J. 1984, A&A, **139**, 15.

Stephan, M. E. 1877, *C. R. Acad. Sci. Paris*, **84**, 641.

van der Hulst, J.M. & Rots, A.H. 1981, AJ, **86**, 1775.

Vigroux, L., Mirabel, F., Altiéri, B. et al. 1996, A&A, **315**, L93.

Yun, M.S., Verdes-Montenegro, L., del Olmo, A. & Perea, J. 1997, ApJ, **475**, 21.

This manuscript was prepared with the AAS LaTeX macros v4.0.

Table 1.

	R.A.	Dec.	Type	v_r	$f_{15\mu}$[1]	H_α[2]	EW(H_α)[3]	K'_{21}[4]
	(J2000)	(J2000)		km/sec	mJy	10^{-13}erg/cm^2/sec	Å	mag
NGC7319	22h36m03.5s	+33d58′33″	SBb (Sy2)	6764	79.8	1.41±0.30	7.6±2.5	10.03
NGC7318a	22h35m56.7s	+33d57′56″	Epec	6630				
NGC7318b	22h35m58.4s	+33d57′58″	SBbc	5774				
NGC7318a/b[5]					19.3	1.08±0.16	5.0±1.2	9.23
NGC7317	22h35m52.0s	+33d56′41″	E	6599	2.1			
NGC7320	22h36m03.5s	+33d56′54″	Sd	786	27.5			10.40
Source A	22h35m58.7s	+33d58′55″	SF region		11.9	1.27±0.13	115±15	15.09
Source B[6]	22h36m10.2s	+33d57′21″	SF region		1.8	0.14±0.01	85±10	

[1]The $15\mu m$ flux density, measured through aperture photometry covering areas included in 2σ contours. The uncertainties are about 30%, dominated by the errors in the calibration.

[2]H_α flux, corrected for the [NIIλ6583/λ6548] contamination. For NGC7319, the Sy2 galaxy, the ratio [NIIλ6583]/H_α = 1.8 is taken from Keel et al. (1985). For other galaxies and star formation regions the [NIIλ6583]/H_α ratio is assumed to be 0.4 (Kennicutt et al. 1994). The errors are dominated by the uncertainties in the continuum subtraction. No extinction correction is applied.

[3]The equivalent line width of the H_α emission, which is the ratio between the H_α flux (in erg/cm^2/sec) and the flux density of the underlying continuum (in erg/cm^2/sec/Å). The continuum is estimated from the R-band flux. For NGC7319 and NGC7318a/b the continuum includes the emission from the entire galaxy and from the galaxy pair, respectively. For Source A, both the H_α flux and the continuum flux density are measured through a rectangular aperture of 30″ × 25″.

[4]K′ ($2.1\mu m$) magnitude measured through isophotal photometry down to K′ = 21 mag/acrsec^2. NGC 7317 is not fully covered by the K′ image. Source B is not detected in K′-band. The errors of the K′ magnitudes are less than 0.2 mag.

[5]The fluxes of this pair of galaxies cannot be separated reliably. Hence they are reported jointly for the pair.

[6]Like Source A, although much fainter, Source B is also a star formation region in the IGM. On the other hand, this source is far away from the shock front and apparently has not been involved in the current collision between NGC7318b and the IGM. Located at the end of one of the tidal tails pointing to NGC7320c (Arp & Lorre 1974), presumably caused by **previous** interactions between SQ and NGC7320c (Moles et al. 1997), Source B is perhaps a star formation condensed out of the tidal tail (Mirabel et a. 1992).

Fig. 1.— ISOCAM LW3 ($15\mu m$) image (false color) of Stephan's Quintet field. The scale is in logarithm and the units are 0.1 mJy/pixel (pixel= $6'' \times 6''$). As shown by the chromatometer, the range of the surface brightness shown in the figure is $-1 \leq \log[S_{15\mu m}/(0.1\ mJy/pixel)] \leq 2$. The five members of the group, including the foreground galaxy NGC7320, are clearly detected. Four other sources outside the galaxies are marked in the image: Source A and Source B are star formation regions associated with the group (see Table 1). Source C is a foreground star, and Source D is a background galaxy.

Fig. 2.— K′ ($2.1\mu m$) image overlaid by contours of the H_α–[NII] emission, covering the same field of sky as in Fig.1. The K′ image is in logarithmic scale. The two components of the H_α–[NII] emission are marked by different colors: the contours of the 6600 km/sec component are in red and those of the 5700 km/sec component in blue. The two contour sets have the same levels, which are 0.3, 0.9, 2.7, 8.1, 24.3 10^{-16} erg/cm^2/sec/pixel (pixel= $0.533'' \times 0.533''$). The first contour level is chosen to hide most of the residuals of the continuum subtraction, the most important source of the errors of the H_α–[NII] maps.

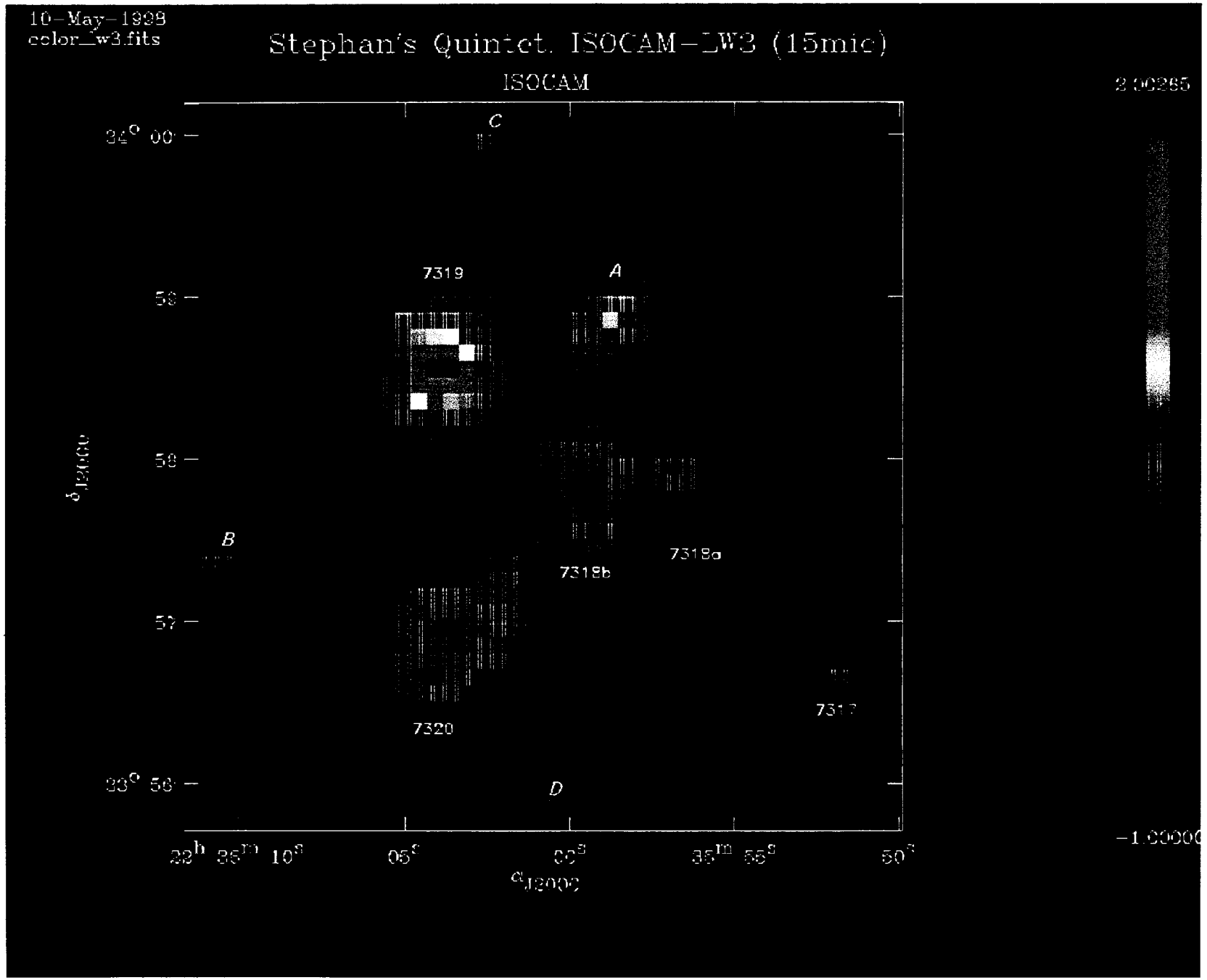
10-May-1998
color_w3.fits
Stephan's Quintet. ISOCAM-LW3 (15mic)
ISOCAM
C
A
B
D
7319
7318a
7318b
7320
34° 00'
58'
56'
54'
52'
33° 58'
22h 35m 10s
05s
00s
34m 55s
50s
δJ2000
αJ2000

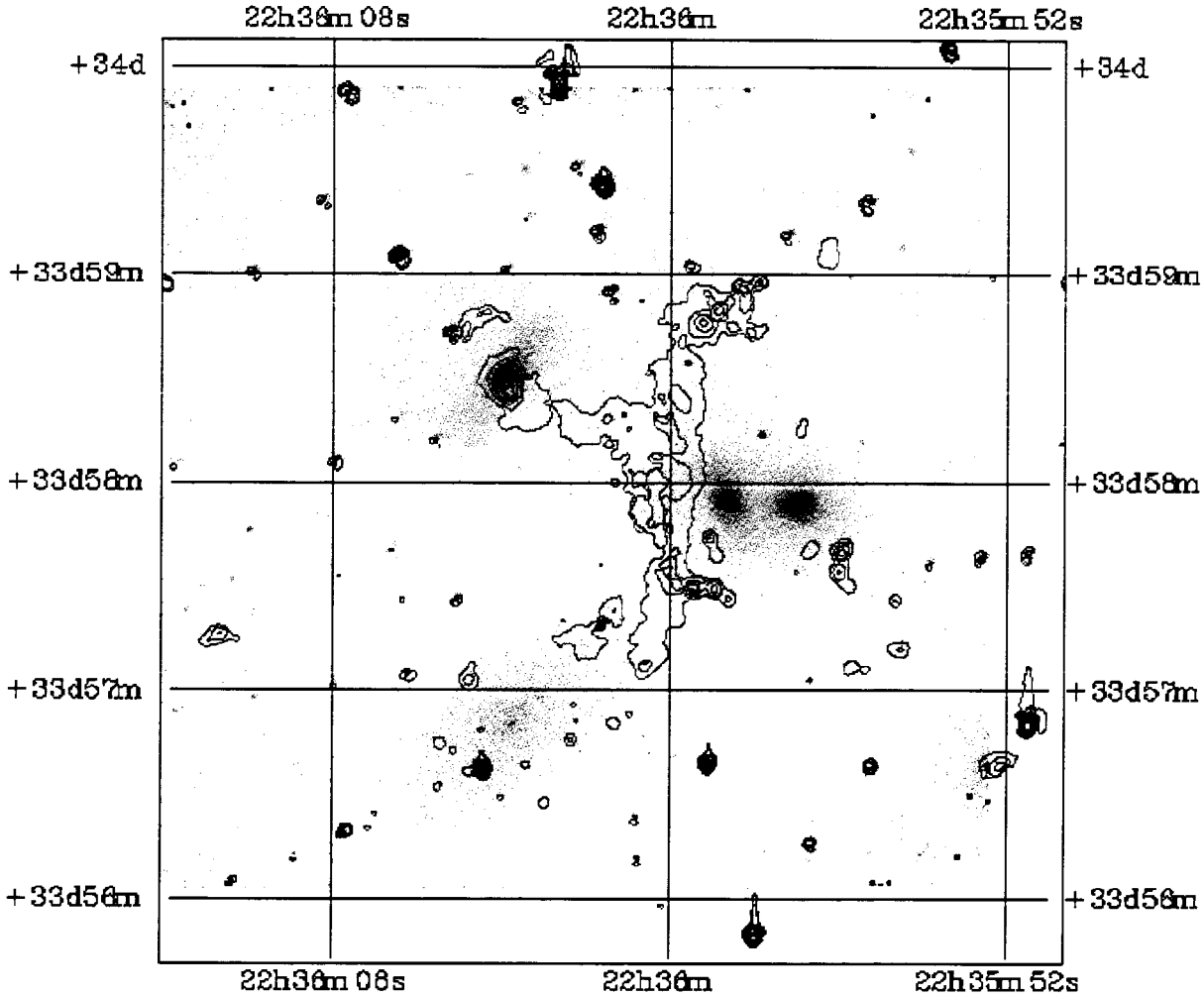
22h36m 08s
22h36m
22h35m 52s
+34d
+33d59m
+33d58m
+33d57m
+33d56m